

A DIAGRAMMATIC PRESENTATION AND ITS CHARACTERIZATION OF NON-SPLIT COMPACT SURFACES IN THE 3-SPHERE

SHOSAKU MATSUZAKI

ABSTRACT. We give a presentation for a non-split compact surface embedded in the 3-sphere S^3 by using diagrams of spatial trivalent graphs equipped with signs and we define Reidemeister moves for such signed diagrams. We show that two diagrams of embedded surfaces are related by Reidemeister moves if and only if the surfaces represented by the diagrams are ambient isotopic in S^3 .

1. INTRODUCTION

A fundamental problem in Knot Theory is to classify knots and links up to ambient isotopy in S^3 . Two knots are equivalent if and only if diagrams of them are related by Reidemeister moves [7]: Reidemeister moves characterize a combinatorial structure of knots. Diagrammatic characterizations for spatial graphs, handlebody-knots and surface-knots are also known, where a spatial graph is a graph in S^3 , a handlebody-knot is a handlebody in S^3 , and a surface-knot is a closed surface in S^4 (cf. [4], [5], [8]). We often use invariants to distinguish the above knots. Many invariants have been discovered on the basis of diagrammatic characterizations. In this paper, we consider presentation of a compact surface embedded in S^3 , which we call a spatial surface. For a knot or link, we immediately obtain its diagram by perturbing the z-axis of projection slightly. For a spatial surface, however, perturbing the spatial surface is not enough to present it in a useful form: it may be overlapped and folded complexly by multiple layers in the direction of the z-axis of $\mathbb{R}^3 \subset S^3$. We will give a diagram for spatial surfaces by using a trivalent spine equipped with information of twisted bands.

If any component of a spatial surface has non-empty boundary, we take a trivalent spine of the surface and take a thin regular neighborhood of the spine; a regular neighborhood of a spine is equivalent to the original spatial surface. In stead of the original surface, we consider the regular neighborhood by using a spatial trivalent graph diagram equipped with information of twisted bands. In Section 3, we give a characterization for spatial surfaces with boundary (Theorems 3.4 and 3.5). The proofs are written in Section 4; we need delicate consideration to avoid difficulty and complexity about information of twisted bands in spatial surfaces. In the process of showing main theorems, we will give a characterization of trivalent spines of surfaces (Theorem 2.1).

When we consider a non-split spatial surface that has closed components, we remove an open disk from each closed component of it; then, we have a spatial surface with boundary. The spatial surface with boundary loses no information up to ambient isotopy after removing an open disk (Proposition 5.1). Therefore, it is sufficient to consider a spatial surface that has boundary when we consider non-split spatial surfaces. We can see some studies for closed surfaces in S^3 in [3], [9] and [10]. Homma defined an unknotted polygon, which is a non-splittable loop of a closed surface embedded in S^3 , and showed that every closed surface in S^3 has an unknotted polygon in [3]. On the base of this fact, Suzuki defined a complexity for a closed surface embedded in 3-manifold and studies it in [9]. Tsukui showed the uniqueness of decompositions for closed genus 2 surfaces in \mathbb{R}^3 in [10]. In those studies, however, we directly deal with closed surfaces without using something like a diagram. We expect developments of those studies by using diagrams of spatial surfaces. On the other hand, we can regard a knot, link or handlebody-knot as a spatial closed surface. This suggests that we can systematically study knots, links and handlebody-knots by the new framework of spatial surfaces (Section 5).

2. AN IH-MOVE FOR TRIVALENT SPINES ON A SURFACE WITH BOUNDARY

We prepare some notations used throughout this paper. We denote by $\#S$ the cardinality of a set S . We denote by $\text{cl}_X(U)$ the closure of a subset U of a topological space X . We denote by ∂M and $\text{int } M$ the boundary and the interior of a topological manifold M , respectively.

We assume that a graph is finite, which has finite edges and vertices. A graph is *trivalent* if every vertex of it is trivalent. A trivalent graph may have a connected component that has no vertices, that is, a trivalent graph may have a circle component. A *surface with boundary* is a compact surface such that every component of it has a non-empty boundary. For a surface F with boundary, a graph G in $F \setminus N_{\partial F}$ is a *spine* of F if N_G and $\text{cl}_F(F \setminus N_{\partial F})$ are ambient isotopic in F , where N_G and $N_{\partial F}$ mean regular neighborhoods of G and ∂F in F , respectively. In this section, we suppose that a surface with boundary has exactly one component.

A disk has no trivalent spines, and an annulus or Möbius band has exactly one trivalent spine up to ambient isotopy, which is a circle. Here we remember that a circle is regarded as a trivalent graph. However, other surfaces with boundary have infinitely many trivalent spines up to ambient isotopy. Theorem 2.1 claims that these spines are related by finitely many *IH-moves*, see Figure 1. Our goal in Section 2 is to prove Theorem 2.1, which gives a characterization of trivalent spines of a surface with boundary.



FIGURE 1. An IH-move: a local replacement of a trivalent spine in a spatial surface with boundary

Theorem 2.1. *Two trivalent spines of a spatial surface are related by finitely many IH-moves and isotopies.*

If a spatial surface F with boundary is a disk, annulus or Möbius band, then a trivalent spine of F is a loop, and two trivalent spines are related by an isotopy of F .

An arc m embedded in a surface F with boundary is *proper* if $m \cap \partial F = \partial m$.

Definition 2.2. Let F and M be a surface with boundary and a disjoint union of proper arcs in F , respectively. Let N_M be a regular neighborhood of M in F . The disjoint union M is a *marking* on F if D is a disk, and the disjoint union $D \cap N_M$ of proper arcs in F consists of exactly three arcs for any connected component D of the closure $\text{cl}_F(F \setminus N_M)$, see Figure 2.

Although a marking M on a surface with boundary is a subset of the surface, we denote by \mathcal{M} the set of connected components of M ; then, an element of \mathcal{M} is a proper arc in F . For a surface F with boundary, there exists a marking on F if and only if F is not a disk, annulus or Möbius band. Other examples of markings are depicted in Figure 5.

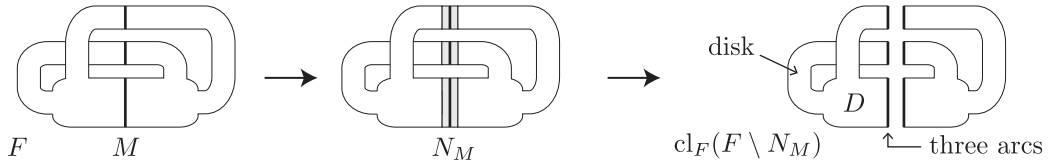


FIGURE 2. A marking M on the closure F of a torus minus a disk

Remark 2.3. If a marking on a surface F with boundary is given, we can construct exactly one trivalent spine of F up to ambient isotopy. Conversely, if a trivalent spine of F is given, we can construct exactly one marking for F up to ambient isotopy.

Lemma 2.4. For markings L and M on a surface F with boundary, it holds that $\#\mathcal{L} = \#\mathcal{M}$.

Proof. By the definition of a marking, we have the equality $2(\#\mathcal{M}) = 3|F \setminus M|$ immediately, where $|F \setminus M|$ means the number of connected components of the topological space $F \setminus M$. We have $\chi(F) = |F \setminus M| - (\#\mathcal{M})$ since F is homotopy equivalent to a graph that has $|F \setminus M|$ vertices and $\#\mathcal{M}$ edges, where $\chi(F)$ is the Euler characteristic of F . Hence, the equality $\#\mathcal{M} = -3\chi(F)$ holds. Therefore, the number of arcs in a marking is determined by the Euler characteristic of surfaces. \square

Let M be a marking on a surface F with boundary. For an arc $m \in \mathcal{M}$, we denote by $D_M(m)$ the connected component of $F \setminus (M \setminus m)$ that contains m . All configurations of $D_M(m)$ are illustrated in Figure 3: the interior $\text{int } D_M(m)$ is an open disk, open annulus, or open Möbius band.

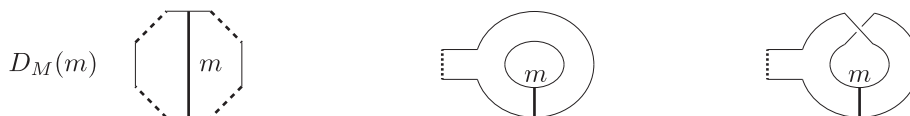


FIGURE 3. All probable configurations of $D_M(m)$

An arc $m \in \mathcal{M}$ is *turnable* if $\text{int } D_M(m)$ is an open disk. For an arc $m \in \mathcal{M}$ and an arbitrary proper arc $m^* \subset F$, we write $M(m, m^*) = (M \setminus m) \sqcup m^*$. Suppose that $m \in \mathcal{M}$ is turnable. For a proper arc $m^* \subset F$ as illustrated in Figure 4, $M(m, m^*)$ is also a marking on F ; $M(m, m^*)$ is said to be obtained from M by *turning* m into m^* , and m is *turned* into m^* .

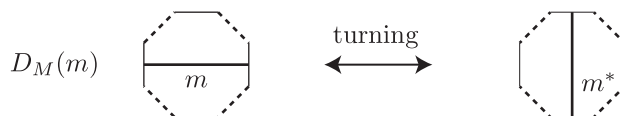


FIGURE 4. Turning a turnable arc

Example 2.5. Let F be a surface with boundary and let L and M be markings on F as illustrated in Figure 5: $\#\mathcal{L} = \#\mathcal{M} = 6$. All arcs in \mathcal{L} are turnable. The arc $m \in \mathcal{M}$ in Figure 5 is not turnable, because $\text{int } D_M(m)$ is an open annulus. The other arcs in \mathcal{M} are turnable. Each trivalent graph in the figure is a trivalent spine of F corresponding to each marking.

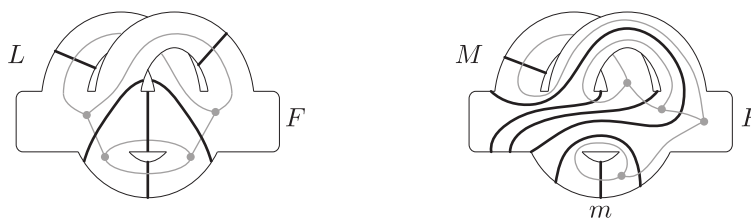


FIGURE 5. Markings are colored by black and the corresponding spines are colored by gray.

Remark 2.6. A turning an arc corresponds to an applying an IH-move of a trivalent spine.

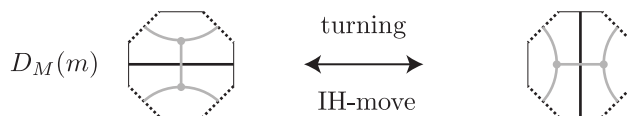


FIGURE 6. Turning a turnable arc corresponds to applying an IH-move.

It can be seen that Theorem 2.1 follows from Theorem 2.7 below by considering Remarks 2.3 and 2.6. We will show Theorem 2.7 instead of proving Theorem 2.1, in this section.

Theorem 2.7. *If L and M are markings on a surface F with boundary, then there exists a finite sequence M_0, M_1, \dots, M_n of markings on F such that*

- M (resp. L) and M_0 (resp. M_n) are ambient isotopic in F , and
- M_i and M_{i+1} are related by turning an arc for any i with $0 \leq i < n$.

We prepare some notations that are needed for the proof of Theorem 2.7. Let L and M be markings on a surface F with boundary such that L intersects M transversally, denoted by $L \bar{\cap} M$. We write

$$\mathcal{W}_L(M) := \{m \in \mathcal{M} \mid m \cap L \neq \emptyset\},$$

$$w_L(M) := \min \{\#\mathcal{W}_L(M') \mid M' \text{ is ambient isotopic to } M \text{ in } F, \text{ and } M' \bar{\cap} L\}.$$

Markings L and M are in *taut position* if there is no disk δ such that δ is bounded by a 2-gon consisting of parts of L and M or by a 3-gon consisting of L , M and ∂F as illustrated in Figure 7. Let $\ell \in \mathcal{L}$ be an arc such that $\ell \cap M \neq \emptyset$. An *endarc* of $(\ell; M)$ (resp. $(L; M)$) is an arc r contained in ℓ (resp. L) such that one point of ∂r is in ∂F and the other point is in M and $\text{int}(r) \cap M = \emptyset$. We note that the number of endarcs of $(L; M)$ is equal to $2 \cdot \#\mathcal{W}_L(M)$. For an endarc r of $(\ell; M)$, we denote by $m(r; M)$ the arc in \mathcal{M} satisfying that $m(r; M)$ has an intersection with r .



FIGURE 7. Two disks bounded by L , M and ∂F

We prepare Lemmas 2.8, 2.9 and 2.10 to show Theorem 2.7.

Lemma 2.8. *Let L and M be markings on a surface F with boundary such that L and M are in taut position. For any endarc r of $(L; M)$, the arc $m(r; M) \in \mathcal{M}$ is turnable.*

Proof. Suppose that $m := m(r; M)$ is not turnable. The configuration of $D_M(m)$ is as illustrated in Figure 8, where we remember that $D_M(m)$ is the connected component of $F \setminus (M \setminus m)$ that contains m . One point of ∂r is in m , and the other point of ∂r is in the boundary of an annulus or a Möbius band as illustrated in Figure 8. In each of the cases, a contradiction occurs for our assumption that L and M are in taut position. Therefore, $m \in \mathcal{M}$ is turnable. \square



FIGURE 8. Two markings in taut position have no nugatory crossings.

Lemmas 2.9 and 2.10 are essential parts for the proof of Theorem 2.7.

Lemma 2.9. *Let L and M be markings on a surface F with boundary satisfying that $w_L(M) = 0$. Then, L and M are ambient isotopic in F .*

Proof. We deform M by an isotopy of F so that $\#\mathcal{W}_L(M) = 0$, that is, $L \cap M = \emptyset$. We take a regular neighborhood N_L of L in F . By an isotopy of F , we move M so that $M \subset N_L$: such an isotopy exists, since L is a marking. We show that each connected component of N_L , which is a disk, contains exactly one arc of \mathcal{M} as a subset and the arc is parallel to an arc of \mathcal{L} .

Let $\ell \in \mathcal{L}$ be an arc, and let N_ℓ be the connected component of N_L that contains ℓ . Since M is a marking, ∂F and any arc $m \in \mathcal{M}$ bound no disks in N_ℓ . Then, m is parallel to ℓ . If N_ℓ contains two and more arcs of \mathcal{M} , the arcs are parallel each other. This leads to a contradiction, since M is a marking. Then, each connected component of N_L contains no arcs of \mathcal{M} or contains exactly one arc of \mathcal{M} . By Lemma 2.4, if a connected component of N_L contains no arcs, this leads to a contradiction with $\#\mathcal{L} = \#\mathcal{M}$. Hence, every connected component of N_L contains exactly one arc, and L and M are parallel. Therefore, L and M are ambient isotopic in F . \square

Lemma 2.10. *Let L and M be markings on a surface F with boundary such that L and M are in taut position and $\#\mathcal{W}_L(M) = w_L(M) > 0$. Then, there is a marking M' such that M' and M are related by finitely many turnings arcs and $w_L(M') < \#\mathcal{W}_L(M)$.*

Proof. In this proof, for any marking N on F , we write $\mathcal{W}(N) = \mathcal{W}_L(N)$ and $w(N) = w_L(N)$ for short notations. Let ℓ be an arc in \mathcal{L} such that $\ell \cap M \neq \emptyset$.

Case 1: we suppose that $\#(\ell \cap M) = 1$.

Let r be an endarc of $(\ell; M)$, and we put $m = m(r; M)$. Since L and M are in taut position, $m \in \mathcal{M}$ is turnable by Lemma 2.8, that is, $\text{int } D_M(m)$ is an open disk. We take a proper arc m^* located along ℓ as illustrated in Figure 9: m^* is close enough to ℓ and $m^* \cap L = \emptyset$, where it may hold that $(L \setminus \ell) \cap M \neq \emptyset$, although $L \setminus \ell$ are not illustrated. By turning m into m^* in $D_M(m)$, we obtain a new marking $M' := M(m, m^*)$ on F . Now, L and M' are in taut position. Then, Any endarc of $(L; M)$ that has no intersections with m is also an endarc of $(L; M')$. Any endarc r' of $(L; M)$ satisfying that $r' \cap m \neq \emptyset$ and $r' \not\subset \ell$ is contained in an endarc of $(L; M')$. Both r and the other endarc of $(\ell; M)$ disappear from M' . Since the number of endarcs of $(L; N)$ is equal to $2 \cdot \#\mathcal{W}(N)$ for any marking N , we have $\#\mathcal{W}(M') = \#\mathcal{W}(M) - 1$; then $\#\mathcal{W}(M') < \#\mathcal{W}(M)$. Since $w(M') \leq \#\mathcal{W}(M')$, we have $w(M') < \#\mathcal{W}(M)$.

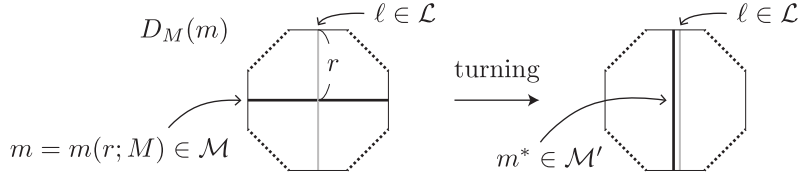


FIGURE 9. Configurations of ℓ , r , m , m^* and $D_M(m)$

Case 2: we suppose that $\#(\ell \cap M) > 1$.

Set $M_0 = M$. Let r_0 be an endarc of $(\ell; M_0)$, and we put $m_0 = m(r_0; M_0)$. Since L and M_0 are in taut position, $m_0 \in \mathcal{M}_0$ is turnable, that is $\text{int } D_{M_0}(m_0)$ is an open disk. Let r_1 be the arc contained in ℓ such that $r_0 \subset r_1$, $\partial(r_1) \subset M_0 \cup F$ and $\#(r_1 \cap M_0) = 2$. Let m_1 the arc in \mathcal{M}_0 such that $\#(m_1 \cap r_1) = 1$ and $m_1 \neq m_0$, see the left in Figure 10.

We take a proper arc m_0^* located partially along ℓ and m_1 as illustrated in the right of Figure 10: m_0^* is close enough to a part of ℓ and m_1 , and there is a possibility that m_0^* has intersections with $\ell \setminus r_1$, although $\ell \setminus r_1$ is not illustrated in Figure 10. By turning m_0 into m_0^* in $D_{M_0}(m_0)$, we have a new marking $M_1 := M_0(m_0, m_0^*)$. Note that r_1 is an endarc of $(\ell; M_1)$, $m_1 = m(r_1; M_1)$ and m_1 is also an arc in \mathcal{M}_1 .

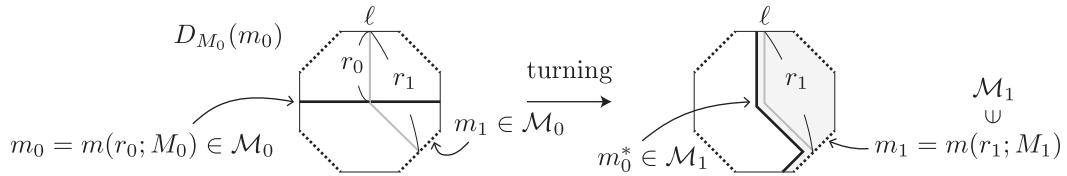


FIGURE 10. Configurations of ℓ , r_0 , r_1 , m_0 , m_1 , m_0^* and $D_{M_0}(m_0)$

We show that (i) $w(M_1) \leq \#\mathcal{W}(M_1) = \#\mathcal{W}(M_0)$ and (ii) $\#(m_0^* \cap \ell) < \#(m_1 \cap \ell)$. Now, L and M_0 are in taut position. Then, by the configuration of m_0^* , any endarc r' of $(L; M_0)$ is also an endarc of $(L; M_1)$, r' contains an endarc of $(L; M_1)$, or r' is contained in an endarc of $(L; M_1)$. Since the number of endarcs of $(L; N)$ is equal to $2 \cdot \#\mathcal{W}(N)$ for any marking N , we have $\#\mathcal{W}(M_1) = \#\mathcal{W}(M_0)$, then (i) holds. The arc r_1 has an intersection with m_1 and has no intersections with m_0^* ; then we have $\#(m_0^* \cap \ell) \leq \#(m_1 \cap \ell) - 1$, that is, (ii) holds.

If the inequality $w(M_1) < \#\mathcal{W}(M_0)$ holds, the proof completes. Then, we suppose that $w(M_1) = \#\mathcal{W}(M_1) = \#\mathcal{W}(M_0)$. Since L and M_1 are also in taut position by the configuration of m_0^* , the arc $m_1 \in \mathcal{M}_1$ is also turnable by Lemma 2.8, that is, $\text{int } D_{M_1}(m_1)$ is an open disk; the shaded region in Figure 10 is a half part of $D_{M_1}(m_1)$. If $\#(m_1 \cap \ell) = 1$, the proof completes by considering Case 1. Then, we suppose that $\#(m_1 \cap \ell) > 1$.

In the same way to construct M_1 , we continue turning arcs along a part of ℓ while keeping L fixed; that is, we recursively define r_i, m_i, m_i^* and a marking $M_{i+1} := M_i(m_i, m_i^*)$ for each integer $i \geq 0$ until it holds that $w(M_n) < \#\mathcal{W}(M_0)$ or $\#(m_n \cap \ell) = 1$ for some integer n . Note that r_i is the endarc of $(\ell; M_i)$ such that $r_{i-1} \subset r_i$, and $m_i = m(r_i; M_i)$, see Figure 11. By the above process, we obtain a sequence $(M_i)_{1 \leq i \leq n}$ of markings satisfying that

$$(i') w(M_i) = \#\mathcal{W}(M_i) = \#\mathcal{W}(M_0) \text{ and } (ii') \#(m_i^* \cap \ell) < \#(m_{i+1} \cap \ell)$$

for any i with $0 \leq i < n$, in the same manner as (i) and (ii).

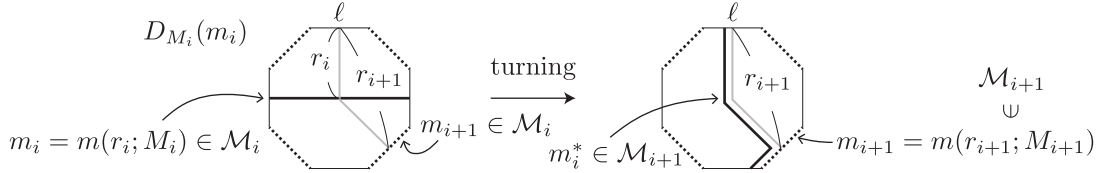


FIGURE 11. Configurations of $\ell, r_i, r_{i+1}, m_i, m_{i+1}, m_i^*$ and $D_{M_i}(m_i)$

It suffices to show that $(M_i)_{1 \leq i \leq n}$ is finite; then we suppose that $(M_i)_{1 \leq i \leq n}$ is infinite. We prepare notations only for this proof. For arcs $\alpha_i \in \mathcal{M}_i$ and $\alpha_j \in \mathcal{M}_j$ with $0 \leq i < j$, we write $\alpha_i \rightarrow \alpha_j$ if $\alpha_i = \alpha_j$ as a subset of F or there is an integer k with $i \leq k < j$ such that $M_k(\alpha_i, \alpha_i^*) = M_{k+1}$ and $\alpha_j = \alpha_i^*$ as a subset of F . For arcs $m \in \mathcal{M}_0$ and $m' \in \mathcal{M}_i$, m' is a descendant of m if there is a finite sequence $\alpha_0, \dots, \alpha_s$ of proper arcs in F such that $\alpha_0 = m$, $\alpha_s = m'$ and $\alpha_j \rightarrow \alpha_{j+1}$ for any j with $0 \leq j < s$. An arc $m \in \mathcal{M}_0$ is *infinite-type* if m continues to be turned endlessly, that is, for any integer i , there exists an integer κ with $\kappa > i$ such that $M_\kappa(m_\kappa, m_\kappa^*) = M_{\kappa+1}$, where $m_\kappa \in \mathcal{M}_\kappa$ is the descendant of m . We put

$$\mathcal{M}_0^\infty = \{m \in \mathcal{M}_0 \mid m \text{ is infinite-type}\}, \text{ and}$$

$$P_i = \{\#(m' \cap \ell) \mid m' \in \mathcal{M}_i \text{ and } m' \text{ is an descendant of an infinite-type arc of } \mathcal{M}_0\},$$

for any integer i , where we define P_i as a multiset, that is, each element of P_i has the multiplicity. Let κ be an integer large enough such that all descendants of $\mathcal{M}_0 \setminus \mathcal{M}_0^\infty$ are no longer turned in \mathcal{M}_i for any i with $\kappa < i$. By the inequality (ii'), after several times turnings, an arc $m \in \mathcal{M}_\kappa$ with $\#(m \cap \ell) = \max P_\kappa$ disappears, and a new arc m' with $\#(m' \cap \ell) < \max P_\kappa$ appears instead. Therefore, there exists an integer k such that $\max P_{\kappa+k} < \max P_\kappa$ or that the multiplicity of $\max P_{\kappa+k}$ is less than that of $\max P_\kappa$, where we remember that P_i is a multiset. Hence, $\max P_{\kappa'}$ is 0 for an integer κ' large enough with $\kappa < \kappa'$. This leads to a contradiction with the infiniteness of $(M_i)_{1 \leq i \leq n}$; then $(M_i)_{1 \leq i \leq n}$ is finite. \square

Proof of Theorem 2.7. Let L and M be markings on a surface F with boundary. If $w_L(M) = 0$, the proof completes by Lemma 2.9; then we assume that $w_L(M) > 0$. By an isotopy of F , we deform M so that L and M are in taut position and $\#\mathcal{W}_L(M) = w_L(M) > 0$. By Lemma 2.10, by finitely many turnings of M , we have a marking M_1 such that $w_L(M_1) < \#\mathcal{W}_L(M)$. By continuing

the same operation, we have a finite sequence M, M_1, \dots, M_n of markings such that $w_L(M_n) = 0$. Therefore, L and M_n are ambient isotopic in F by Lemma 2.9. \square

3. A DIAGRAM OF A SPATIAL SURFACE WITH BOUNDARY

We regard S^3 as the one-point compactification $\mathbb{R}^3 \cup \{\infty\}$ of the Euclidean space \mathbb{R}^3 . We regard \mathbb{R}^2 as the set $\{(x, y, z) \in \mathbb{R}^3 | z = 0\}$ and regard S^2 as $\mathbb{R}^2 \cup \{\infty\}$. Note that $\mathbb{R}^2 \subset \mathbb{R}^2 \cup \{\infty\} = S^2 \subset \mathbb{R}^3 \cup \{\infty\} = S^3$. Let $\text{pr} : \mathbb{R}^3 \rightarrow \mathbb{R}^2; (x, y, z) \mapsto (x, y, 0)$ be the canonical projection.

An *spatial surface* is a compact surface embedded in S^3 . A *spatial closed surface* is a spatial surface that is a closed surface. A *spatial surface with boundary* is a spatial surface that is a surface with boundary. A spatial surface that has n connected components is said to be *n-component*. In Sections 3 and 4, we call a spatial surface with boundary a spatial surface for short, unless we note otherwise. If a spatial surface has intersection with ∞ , we can deform the spatial surface so that it is contained in $\mathbb{R}^3 = S^3 \setminus \{\infty\}$ by perturbation around $\{\infty\}$; then we assume that a spatial surface contained in \mathbb{R}^3 . A disk embedded in S^3 is unique up to ambient isotopy; then we assume that a spatial surface has no disk components throughout this paper.

For the same reason as the case of spatial surfaces, we assume that a spatial graph is contained in \mathbb{R}^3 . A spatial graph G is in *semiregular position* with respect to pr if it satisfies that

- $\text{pr}(G)$ has finitely many multiple points, that is, $\{p \in \text{pr}(G) | \#(G \cap \text{pr}^{-1}(p)) \geq 2\}$ is finite,
- any multiple point $p \in \text{pr}(G)$ is a double point, that is, $\#(G \cap \text{pr}^{-1}(p)) = 2$,
- $\text{pr}(v) \in \text{pr}(G)$ is not a double point for any vertex of G .

For a spatial graph G in semiregular position, a double point $p \in \text{pr}(G)$ is *regular* if there are two disjoint open intervals I and I' in G such that $\text{pr}(I)$ and $\text{pr}(I')$ intersect transversally at p . A double point $p \in \text{pr}(G)$ is *non-regular* if p is not regular. A spatial graph G is in *regular position* with respect to pr if it satisfies that

- G is in semiregular position with respect to pr , and
- every double point p of $\text{pr}(G)$ is regular.

A *projection* of spatial graphs is the image $\text{pr}(G)$ of a spatial graph G in regular position. A *spatial graph diagram* is a pair of a projection of spatial graphs and under/over information at every double point. For a spatial graph G in regular position, we denote by $D(G)$ the spatial graph diagram satisfying that the projection of $D(G)$ is $\text{pr}(G)$ and that the under/over information at each double point is directly obtained from G .

We denote by $V_n(G)$ the set of n -valent vertices of a graph G . In this paper, we regard a spatial graph diagram D as a graph; we denote by $V_n(D)$ the set of n -valent vertices of D . A *2, 3-graph* is a graph whose any vertex is bivalent or trivalent. Note that a trivalent graph is a kind of 2,3-graph.

Definition 3.1. For a spatial 2, 3-graph diagram D , we call a map $s : V_2(D) \rightarrow \{\pm 1\}$ a *sign* of D . A *spatial surface diagram* is a pair (D, s) of a spatial 2,3-graph diagram D and a sign s of D .

Although spatial trivalent graph diagram D has no bivalent vertices, we regard the empty function $\emptyset_{\{\pm 1\}} : V_2(D) \rightarrow \{\pm 1\}$ as a sign of D . For a spatial surface diagram $D := (D, s)$, we construct an unoriented spatial surface $\text{Sf}(D)$ by operations as illustrated in Figure 12: an arc is replaced with a band, a bivalent vertex is replaced with a twisted band, and one of two crossed bands is slightly perturbed into the direction of the z-axis around each crossing. An example of a spatial surface diagram D and its spatial surface $\text{Sf}(D)$ is illustrated in Figure 13.

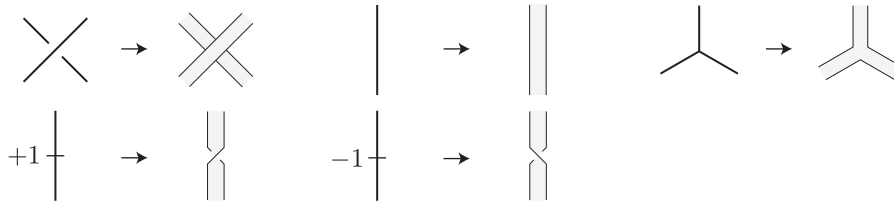
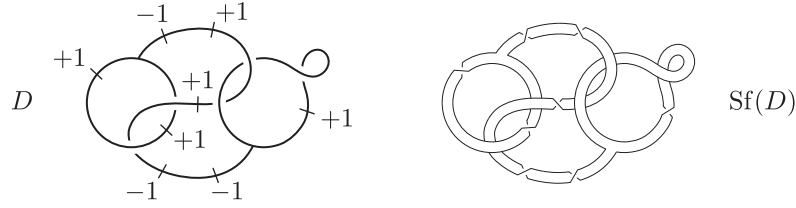


FIGURE 12. Operations for spatial surface diagrams

FIGURE 13. A spatial surface diagram D and its spatial surface $\text{Sf}(D)$

Definition 3.2. The *Reidemeister moves* for a spatial surface are defined as illustrated in Figure 14: each area outside of a dotted circle is not changed before and after the replacement.

Spatial surface diagrams D and D' are said to be *related* by R0–R6 moves in \mathbb{R}^2 (resp. S^2) if there exists a finite sequence $(D_i)_{1 \leq i \leq n}$ of spatial surface diagrams with $D_1 = D$ and $D_n = D'$ such that D_i is transformed into D_{i+1} by one of R0–R6 moves in \mathbb{R}^2 (resp. S^2) for any i .

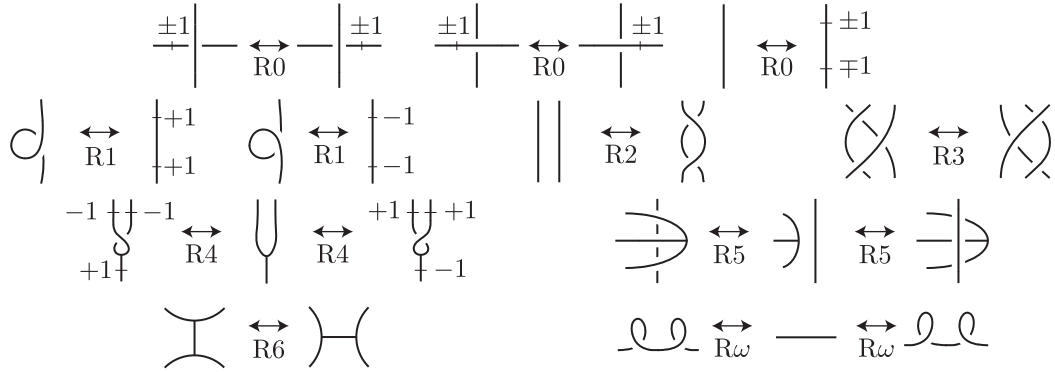


FIGURE 14. Reidemeister moves for a spatial surface diagram.

Remark 3.3. An $R\omega$ move is realized by using R0 and R1 moves.

As is mentioned in Lemma 4.1 (1), for an arbitrary unoriented spatial surface F , there is a spatial surface diagram $D := (D, s)$ such that $\text{Sf}(D)$ and F are ambient isotopic in S^3 , where we call D a *diagram* of F , hereafter. Theorems 3.4 and 3.5 below are main theorems in this paper.

Theorem 3.4. Let D and D' be diagrams of unoriented spatial surfaces F and F' , respectively. Then, the following conditions are equivalent:

- F and F' are ambient isotopic in S^3 .
- D and D' are related by R0–R6 moves in \mathbb{R}^2 .

Next, we consider oriented spatial surfaces. Let D be a spatial surface diagram with no bivalent vertices; $\text{Sf}(D)$ is orientable. We give an orientation for $\text{Sf}(D)$ as illustrated in Figure 15: a side of F facing the positive direction of the z-axis is defined as a front side and the other side of F is defined as a back side. We denote by $\vec{\text{Sf}}(D)$ the spatial surface $\text{Sf}(D)$ equipped with the above-mentioned orientation.

As is mentioned in Lemma 4.1 (2), for any oriented spatial surface F , there is a spatial surface diagram D with no bivalent vertices such that $\vec{\text{Sf}}(D)$ and F are ambient isotopic in S^3 including orientations, where we call D a *diagram* of F , hereafter.



FIGURE 15. A spatial surface diagram D with no bivalent vertices, and $\vec{\text{Sf}}(D)$

Theorem 3.5. *Let D and D' be diagrams of oriented spatial surfaces F and F' , respectively. Then, the following conditions are equivalent.*

- (a) F and F' are ambient isotopic in S^3 including orientations.
- (b) D and D' are related by $R\omega$, $R2$ – $R3$ and $R5$ – $R6$ moves in \mathbb{R}^2 .
- (c) D and D' are related by $R2$ – $R3$ and $R5$ – $R6$ moves in S^2 .

The proofs of Theorems 3.4 and 3.5 are written in Section 4. When we deal with a spatial surface that contains closed components, we consider a spatial surface with boundary that is obtained by removing an open disk in each closed component. Details are described in Section 5.

Remark 3.6. A ribbon surface is studied in [1], [2], which is a surface with boundary properly embedded in the 4-ball B^4 . A ribbon surface is presented by a “1-diagram”, which corresponds to a spatial surface diagram. Two ribbon surfaces are “1-isotopic” if and only if their 1-diagrams are related by some local replacements which contain Reidemeister moves in Figure 14.

4. THE PROOFS OF THEOREMS 3.4 AND 3.5

Throughout Section 4, a bivalent vertex v of a spatial surface diagram $D := (D, s)$ is denoted by a black (resp. white) vertex if $s(v) = +1$ (resp. $s(v) = -1$), see Figure 16. A spatial surface $\text{Sf}(D)$ is already defined in Definition 3.1. However, in Section 4, we replace each bivalent vertex with the band as illustrated in Figure 16 to avoid complication of figures: twisted bands in Figure 16 and Figure 12 are ambient isotopic in a local area.



FIGURE 16. A black/white vertex and a twisted band

We prepare some notations used in proofs. Let D and G be a spatial surface diagram and a trivalent spine of $F := \text{Sf}(D)$, respectively. A proper arc α in F is a *corner-arc* if the restriction $\text{pr}|_{N_p}$ is not injective for any neighborhood N_p of any point $p \in \alpha$, see Figure 17. We denote by A_F the disjoint union of corner-arcs of F . The pair $(G; F)$ is in *semiregular position* if

- G , which is a spatial graph, is in semiregular position (see Section 3), and
- the set $G \cap A_F$ is finite, that is, G has intersection with A_F at finitely many points.

Suppose that $(G; F)$ is in semiregular position. A point $p \in A_F \cap G$ is *transversal* if A_F and G intersect transversally at p . A point $p \in A_F \cap G$ is *non-transversal* if p is not transversal. A trivalent vertex is non-transversal if it is in A_F . The pair $(G; F)$ is in *regular position* if

- the spatial trivalent graph G is in regular position (see Section 3),
- $(G; F)$ is in semiregular position and any point in $A_F \cap G$ is transversal.

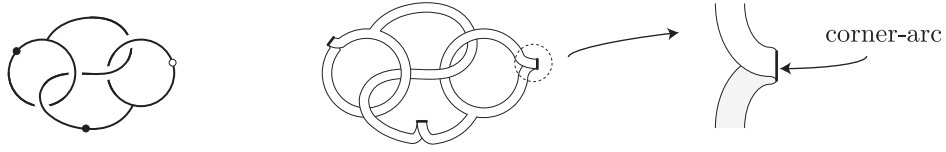


FIGURE 17. Thick proper arcs mean corner-arcs of $F(D)$.

Suppose that $(G; F)$ is in regular position. We explain a way to construct a spatial surface diagram $D(G; F)$. First, we replace every point in $G \cap A_F$ with a bivalent vertex. We regard G as the spatial 2,3-graph obtained by adding bivalent vertices. Next, we define a sign $s(G; F)$ of $D(G)$. We fix a “thin” regular neighborhood N_G of G in F ; N_G and F are ambient isotopic in $\mathbb{R}^3 \subset S^3$. For every bivalent vertex v in $D(G)$, which is on a corner-arc of F , we define $s(G; F)(v)$ by observing a peripheral area around v as depicted in Figure 18. Then, we have the spatial surface diagram $(D(G), s(G; F))$, denoted by $D(G; F)$ hereafter.

We also write $\text{Sf}(G; F) = \text{Sf}(D(G; F))$. We often assume that $\text{Sf}(G; F)$ is in F , that is, we identify $\text{Sf}(G; F)$ with N_G .

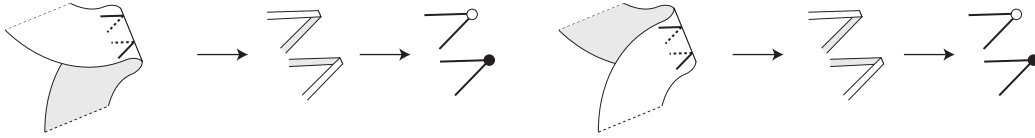


FIGURE 18. Procedure for obtaining the sign $s(G; F)$ of $D(G)$

The lemma below claims that any spatial surface can be presented by spatial surface diagrams.

Lemma 4.1. *Let F be an spatial surface.*

- (1) *There is a spatial surface diagram D such that $\text{Sf}(D)$ and F are ambient isotopic in S^3 .*
- (2) *If F is orientable and oriented, then there is a spatial surface diagram D with no bivalent vertices such that $\vec{\text{Sf}}(D)$ and F are ambient isotopic in S^3 including orientations.*

Proof. We describe an example of ways to construct a diagram of F .

We prove (1). By perturbing F slightly, we deform F so that $\text{pr}|_U$ is injective for some open subset U of F . We fix an arbitrary trivalent spine G of F . By an isotopy of F , we deform G so that every trivalent vertex of G is contained in U . We perturb the z -axis of the canonical projection pr slightly so that G is in regular position. Next, we take a thin enough neighborhood N_G of G in F . If necessary, we deform any twisted part of N_G into the configuration in Figure 16 so that $(G; N_G)$ is in regular position. Since N_G and F are ambient isotopic, $\text{Sf}(G; N_G)$ and F are ambient isotopic, where we regard $\text{Sf}(G; N_G)$ as N_G .

We prove (2). By the consequence of (1), there is a spatial $D := (D, s)$ such that $\text{Sf}(D)$ and F are ambient isotopic, where we forget the orientation of F . Let G be a 2,3-spine of F such that $D(G) = D$. By an isotopy of S^3 , we deform the oriented surface F so that any front side of peripheral regions around trivalent vertices of G faces the positive direction of the z -axis. By an isotopy of S^3 that keeps any peripheral region of trivalent vertices fixed, we deform all full twisted bands as illustrated in Figure 19. Then, we obtain a spatial surface diagram D' with no bivalent vertices such that $\vec{\text{Sf}}(D')$ and F are ambient isotopic in S^3 including orientations. \square



FIGURE 19. A full twist band is deformed into a teardrop-like band.

4.1. **The proof of Theorem 3.4.** For also spatial trivalent graph diagrams, Reidemeister moves are defined as illustrated in Figure 20 (cf. [5]). Two spatial trivalent graph diagrams are related by Reidemeister moves if and only if the two spatial graphs are ambient isotopic in S^3 . We use the same symbols as the spatial surface diagrams; an R2, R3 or R5 move of Figure 20 is the same as that of Figure 14.

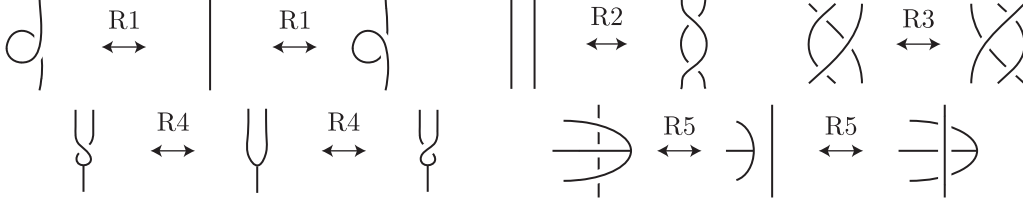


FIGURE 20. Reidemeister moves for spatial trivalent graph diagrams

For a spatial surface diagram D , let us denote by \overline{D} the spatial trivalent graph diagram that is obtained from D by forgetting its bivalent vertices. A spatial surface F is *well-formed* if $F = \text{Sf}(D)$ for some spatial surface diagram D , where this notation is used only in Lemma 4.2.

Lemma 4.2. *Let D be a spatial surface diagram, and we put $F = \text{Sf}(D)$. We denote by G the trivalent spine of F satisfying $D(G; F) = D$. Let $\{h_t : \mathbb{R}^3 \rightarrow \mathbb{R}^3\}_{t \in [0,1]}$ be an isotopy with $h_0 = \text{id}_{\mathbb{R}^3}$ such that $h_1(F)$ is well-formed and that $(h_1(G); h_1(F))$ is in regular position. Then, D and $D(h_1(G); h_1(F))$ are related by R0–R5 moves in \mathbb{R}^2 .*

Proof. For any subset X in \mathbb{R}^3 and any $t \in [0, 1]$, we write $X_t = h_t(X)$. We slightly perturb the z -axis of the canonical projection pr so that the following conditions are satisfied:

- the trivalent spatial graph G_t is in regular, otherwise semiregular position for any $t \in [0, 1]$,
- the set $P := \{t \in [0, 1] \mid G_t \text{ is not in regular position}\}$ is finite, and
- if $t \in P$, then $\text{pr}(G_t)$ has exactly one non-regular double point.

Set $I = [0, 1] \setminus P$, where we note that G_t is in regular position for any $t \in I$. For any $t \in I$, we write $E_t = D(G_t)$, which is a spatial trivalent graph diagram. Note that $E_0 = \overline{D}$ and $E_1 = \overline{D(h_1(G); h_1(F))}$. Let p_1, p_2, \dots, p_n be all points in P such that $p_1 < \dots < p_n$, where we put $n = \#P$. We put $I_i = \{t \in [0, 1] \mid p_i < t < p_{i+1}\}$ for any integer i with $0 \leq i \leq n$, where we set $p_0 = 0$ and $p_{n+1} = 1$.

By adding bivalent vertices and signs to the sequence $(E_t)_{t \in I}$ of spatial trivalent graph diagrams, we will construct a sequence $(D_t)_{t \in I}$ of spatial surface diagrams with $D = D_0$ such that D_{t_i} and $D_{t_{i+1}}$ are related by R0–R5 moves for any i with $1 \leq i < n$ and any $t_i \in I_i$ and $t_{i+1} \in I_{i+1}$. Furthermore, we will show that D_1 and $D(h_1(G); h_1(F))$ are related by R0 moves; then the proof will complete.

First, we recursively construct a sequence $(D_t)_{t \in I}$ satisfying $\overline{D}_t = E_t$ for any $t \in I$. We set $D_0 = D$. We define D_{t_0} for any $t_0 \in I_0$ as follows: D_{t_0} and D_0 are related by an isotopy of \mathbb{R}^2 and $\overline{D}_{t_0} = E_{t_0}$. Suppose that $(D_t)_{t \in I_0 \cup \dots \cup I_i}$ is already defined. We define $(D_t)_{t \in I_0 \cup \dots \cup I_{i+1}}$ by the following procedures.

Case 1: we consider the case where an R1 (resp. R4) move of Figure 20 is applied at p_{i+1} in the sequence $(E_t)_{t \in I}$. Let δ be a small region in which the move is applied. If a bivalent vertex of the corresponding spatial surface diagram is contained in δ , we move the vertex on the outside of δ by using R0 moves. By adding bivalent vertices, we define $D_{t_{i+1}}$ for any $t_{i+1} \in I_{i+1}$ as illustrated in Figure 21: R0 and R1 (resp. R4) moves of Figure 14 are applied before and after p_{i+1} , $\overline{D}_{t_{i+1}} = E_{t_{i+1}}$, and $D_{t_{i+1}}$ and $D_{t'_{i+1}}$ are related by R0 moves and an isotopy of \mathbb{R}^2 for any $t'_{i+1} \in I_{i+1}$. The case of applying the right R1 (resp. R4) move of Figure 20 is omitted.

Case 2: we consider the case a move except for both R1 and R4 moves of Figure 20 is applied at p_{i+1} in the sequence $(E_t)_{t \in I}$. Let δ be a small region in which the move is applied. If a bivalent vertex of the corresponding spatial surface diagram is contained in δ , we move it on the outside

of δ by R0 moves. By adding no bivalent vertices, we define $D_{t_{i+1}}$ for any $t_{i+1} \in I_{i+1}$ as follows: $D_{t_{i+1}}$ is equal to $E_{t_{i+1}}$ in δ , $\overline{D_{t_{i+1}}} = E_{t_{i+1}}$, and $D_{t_{i+1}}$ and $D_{t'_{i+1}}$ are related by R0 moves and an isotopy of \mathbb{R}^2 for any $t'_{i+1} \in I_{i+1}$. Before and after p_{i+1} , a move that is not illustrated in Figure 20 may be applied, however, D_{t_i} and $D_{t_{i+1}}$ are actually related by R2, R3 and R5 moves; two examples of a move that is not illustrated in Figure 20 are depicted in Figure 22.

By the above processes, we have a sequence $(D_t)_{t \in I}$ of spatial surface diagrams satisfying that $\overline{D_t} = E_t$ for any $t \in I$; then D and D_1 are related by R0–R5 moves.

Secondly, we show that D_1 and $D(h_1(G); h_1(F))$ are related by R0 moves, where we note that $D(G_1; F_1) = D(h_1(G); h_1(F))$. We take a thin enough regular neighborhood V of G in \mathbb{R}^3 so that $F'_t := V_t \cap F_t$ is a regular neighborhood of G_t in F_t for any $t \in [0, 1]$. Now, V_t is a disjoint union of handlebodies embedded in \mathbb{R}^3 , and F'_t is a spatial surface properly embedded in V_t , that is, $\partial F'_t \subset \partial V_t$ and $\text{int } F'_t \subset \text{int } V_t$.

Although each F'_t is properly embedded in V_t , we regard that each $\text{Sf}(D_t)$ is also properly embedded in V_t and that $\text{Sf}(D_t)$ contains G_t for any $t \in I$, where we note that G_t is also a spine of $\text{Sf}(D_t)$. We regard that $F'_1 = \text{Sf}(G_1; F_1)$. By the construction of $(\text{Sf}(D_t))_{t \in I}$, the spatial surfaces $\text{Sf}(D_1)$ and F'_1 are related by an isotopy $\{\varphi_t : V_1 \rightarrow V_1\}_{t \in [0, 1]}$ satisfying that $\varphi_0 = \text{id}|_{V_1}$, $\varphi_1(\text{Sf}(D_1)) = F'_1$ and $\varphi_t(x) = x$ for any $t \in I$ and any $x \in G_1$. Let e be an edge of G_1 . Since $\{\varphi_t\}_{t \in [0, 1]}$ keeps G_1 fixed, then there exist bands $B := e \times J \subset \text{Sf}(D_1)$ and $B' := e \times J' \subset F'_1$ such that $\varphi_1(B) = B'$ and $e \subset \partial e \times J = \partial e \times J' \subset G_1$, where each of J and J' is a closed interval. An example of B is illustrated in Figure 23.

The sum of the sign of vertices on $\text{pr}(e)$ in D_1 is equal to that in $D(G_1; F_1)$. Therefore, D_1 and $D(G_1; F_1)$ are related by R0 moves. \square

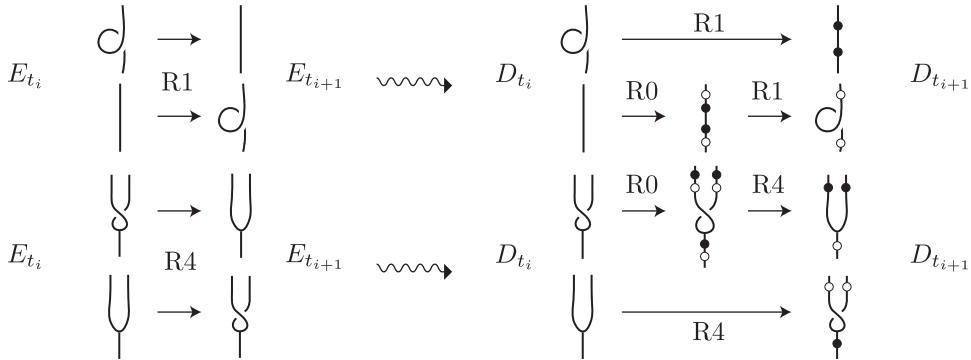


FIGURE 21. Applying R0 and R1 (resp. R4) moves of spatial surface diagrams

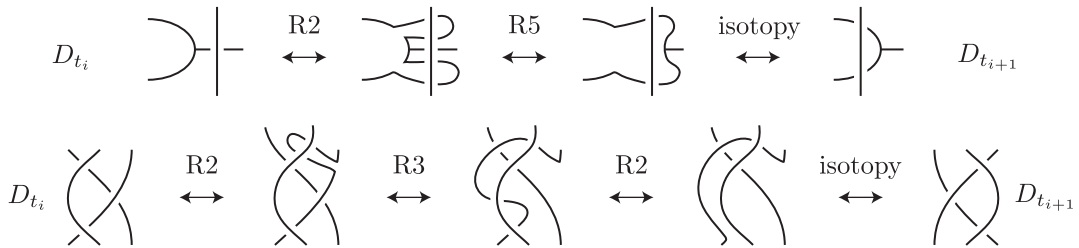


FIGURE 22. Deformations by using R2, R3 and R5

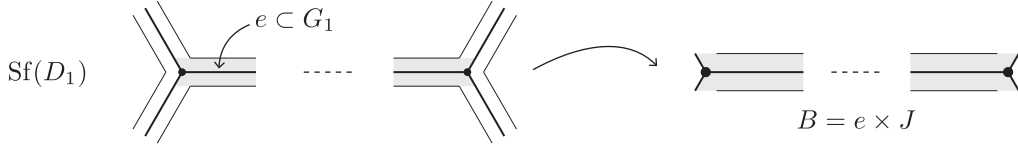


FIGURE 23. A band $B = e \times J$, where J is a segment homeomorphic to $[0, 1]$.

Lemma 4.3. *Let D be a spatial surface diagram, and put $F = \text{Sf}(D)$. Let G be a trivalent spine of F such that $(G; F)$ is in regular position. Then,*

- (1) $D(G; F)$ and D are related by R0–R6 moves in \mathbb{R}^2 , and
- (2) $D(G; F)$ and D are related by R2–R3, R5–R6 moves in \mathbb{R}^2 , if D has no bivalent vertices.

Proof. We show (1). Let G_0 be the spine of F satisfying $D(G_0; F) = D$. Since two trivalent spines are related by finitely many IH-moves and isotopy (Theorem 2.1), it suffices to show that D and $D(G; F)$ are related by R0–R6 moves if G_0 and G are related by exactly one IH-move or an isotopy in F .

First, we suppose that G_0 and G are related by an isotopy in F ; we show that D and $D(G; F)$ are related by R0–R5 moves. Let $\{h_t : F \rightarrow F\}_{t \in [0,1]}$ be an isotopy of F with $h_0 = \text{id}|_F$ such that $h_1(G_0) = G$. Write $G_t = h_t(G_0)$ for any $t \in [0, 1]$. We set $P = \{t \in [0, 1] \mid (G_t; F) \text{ is not in regular position}\}$. We slightly perturb the z-axis of pr so that the following conditions are satisfied.

- The pair $(G_t; F)$ is in regular, otherwise semiregular position for any $t \in [0, 1]$.
- The set $P := \{t \in [0, 1] \mid (G_t; F) \text{ is not in regular position}\}$ is finite.
- For any $t \in P$,
 - the projection $\text{pr}(G_t)$ has exactly one non-regular double point, and any intersection of G_t with A_F is transversal, otherwise
 - the spatial graph G_t has exactly one non-transversal intersection with A_F , and any double point of $\text{pr}(G_t)$ is regular.

Put $I = [0, 1] \setminus P$. For any $t \in I$, $(G_t; F)$ is in regular position; $D(G_t; F)$ is well-defined. We check the sequence $(D(G_t; F))_{t \in I}$ of spatial surface diagrams in detail. Let p be a point in P .

Case 1: we consider the case where G_p has a non-transversal intersection v with A_F such that v is not a trivalent vertex. Before and after p in $(D(G_t; F))_{t \in I}$, one of the deformations in Figure 24 is applied, although the case where an arc passes through a corner-arc from the back side of F is omitted. Each deformation is realized by R0–R1 moves.

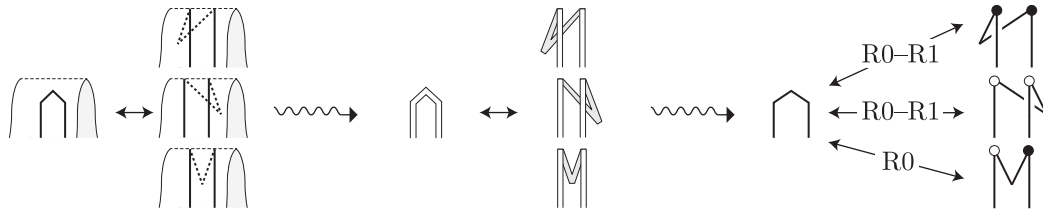


FIGURE 24. Processes that an arc passes through a corner-arc from the front side

Case 2: we consider the case where G_p has a non-transversal intersection with A_F such that v is a trivalent vertex in A_F . Before and after p in $(D(G_t; F))_{t \in I}$, one of the deformations in Figure 25 is applied, although the case where a vertex passes through a corner-arc from the back side of F is omitted. Each deformation is realized by R0 and R4 moves.

Case 3: we consider the case where $\text{pr}(G_p)$ has a non-regular double point. Note that $(D(G_t))_{t \in I}$ is a sequence of spatial trivalent graph diagrams. Since no arcs pass through a corner-arc before and after p , then an R0 move is not applied before and after p in $(D(G_t))_{t \in I}$. Since no trivalent vertices pass through a corner-arc before and after p , then an R4 move is not applied in

$(D(G_t))_{t \in I}$ before and after p . Suppose that an R1 move is applied in $(D(G_t))_{t \in I}$ before and after p . Since no arcs pass through a corner arc before and after p , one of the deformations in Figure 26 is applied in $(D(G_t; F))_{t \in I}$ before and after p . Each deformation is realized by R0–R1 moves. If an R1 move is not applied before and after p in $(D(G_t))_{t \in I}$, two spatial surface diagrams are related by R2, R3 and R5 moves before and after p in $(D(G_t; F))_{t \in I}$.

By considering the cases above, D and $D(G; F)$ are related by R0–R5 moves, where we note $D = D(G_0; F)$ and $D(G; F) = D(G_1; F)$.

Secondly, we suppose that G_0 and G are related by an IH-move on F ; we show that D and $D(G; F)$ are related by R0–R6 moves. When an IH-move is applied, there might be many arcs above or below the region where the IH-move is applied. Then, we shrink the region, by isotopy of F , into a small region so that an R6 move can be applied. In the process of shrinking the region, R0–R5 moves are applied: the first case. Hence, D and $D(G; F)$ are related by R0–R6.

We show (2). Since F has no corner-arcs, none of R0–R1 and R4 moves are not applied, see the case 1. Therefore, D and $D(G; F)$ are related by R2–R3 and R5–R6 moves. \square

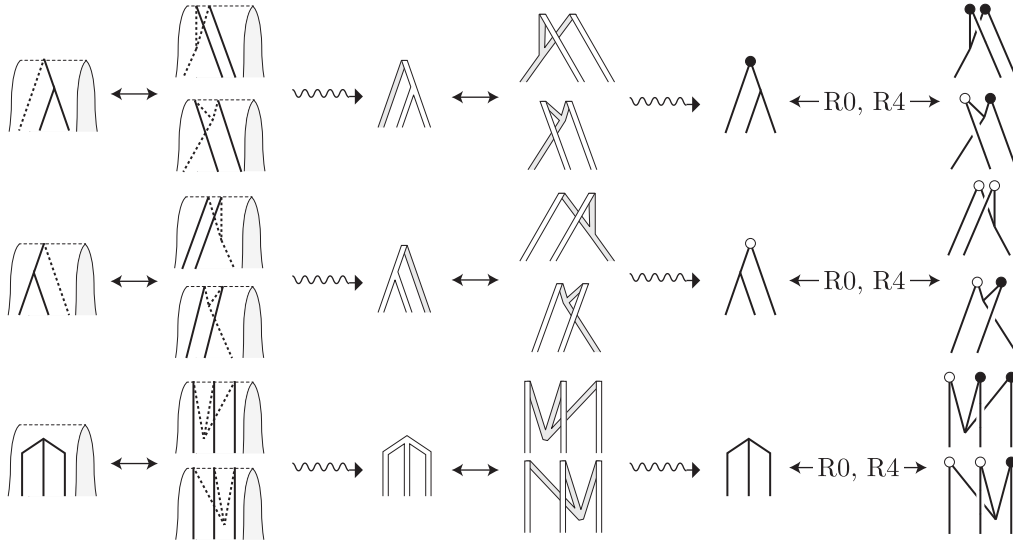


FIGURE 25. Processes that a trivalent vertex passes through a corner-arc from the front side.

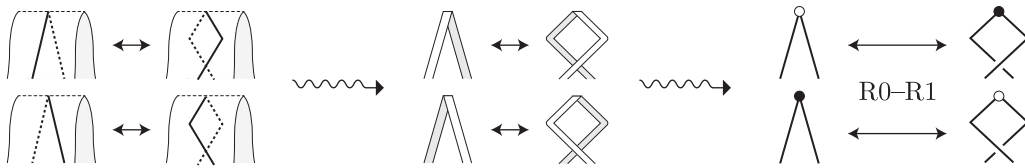


FIGURE 26. All deformations around a corner-arc

Proof of Theorem 3.4. Since F and $\text{Sf}(D)$ are ambient isotopic, we assume that $\text{Sf}(D) = F$. For the same reason, we assume that $\text{Sf}(D') = F'$.

Suppose that (b) is satisfied. If D and D' are related by exactly one of R0–R6 moves, we can immediately construct an isotopy between F and F' . Since D and D' are related by finitely many R2–R3 and R5–R6 moves, then F and F' are also ambient isotopic; (a) holds.

Suppose that (a) is satisfied; we show that (b) holds. Let G (resp. G') be the trivalent spine of F (resp. F') such that $D(G; F) = D$ (resp. $D(G'; F') = D'$). Since F and F' are ambient isotopic, we take an isotopy $\{h_t : \mathbb{R}^3 \rightarrow \mathbb{R}^3\}_{t \in [0,1]}$ with $h_0 = \text{id}|_{\mathbb{R}^3}$ such that $h_1(F) = F'$ and

$(h_1(G); h_1(F))$ is in regular position. By Lemma 4.2, D and $D(h_1(G); h_1(F))$ are related by R0–R5 moves. Furthermore, $D(h_1(G); h_1(F))$ and D' are related by R0–R6 moves by Lemma 4.3 (1). Therefore, D and D' are related by R0–R6 moves. \square

4.2. The proof of Theorem 3.5.

Lemma 4.4. (1) *The local replacement in Figure 27 is realized by R2–R3 moves in the shaded region of the figure.*



FIGURE 27. A local replacement

(2) *If a spatial surface diagram D has no bivalent vertices, then an $R\omega$ move as illustrated in Figure 14 is realized by R2–R3 and R5 moves on S^2 .*

Proof. We show (1). The left local replacement in Figure 27 is realized by R2–R3 moves on \mathbb{R}^2 as depicted in Figure 28. The right replacement in Figure 27 is also realized by R2–R3 moves in the same manner.



FIGURE 28. This deformation is realized by R2–R3 moves in \mathbb{R}^2 .

We show (2). When the thick part of the arc in Figure 29 is passing through the backside of the sphere S^2 , R2–R3 and R5 moves are applied. The right $R\omega$ move in Figure 14 is also realized by the same moves. \square

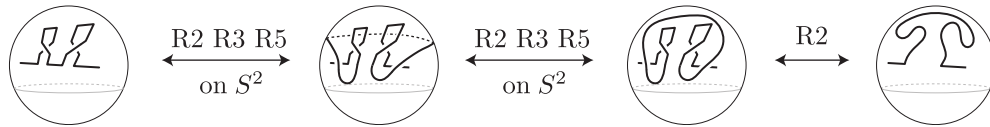


FIGURE 29. The $R\omega$ move is realized by R2–R3 and R5 moves in S^2 .

For a spatial surface diagram D , let us denote by \bar{D} the spatial surface diagram that is obtained from D by forgetting its bivalent vertices: \bar{D} has no bivalent vertices, and the sign of \bar{D} is the empty function. We call an edge of \bar{D} an *edge of D* for a simplicity notation. A self-crossing of D is *positive* (resp. *negative*) if it is the left (resp. right) self-crossing of Figure 30: a dashed line may have crossings with other arcs of D .



FIGURE 30. A positive self-crossing and a negative self-crossing

Definition 4.5. For an edge e of a spatial surface diagram (D, s) , let us denote by $p(e)$ and $n(e)$ the number of positive and negative self-crossings of e , respectively. We define the *framing* $f(e)$ of e as $f(e) = 2(p(e) - n(e)) + s(e)$, where we write $s(e) = \sum_{v \in V_2(D) \cap e} s(v)$.

Lemma 4.6. *If we apply R0–R3 moves for a spatial surface diagram, the framing of each edge does not change.*

Proof. We can check easily that the framing of each edge does not change before and after an R0, R1, R2 or R3 move. \square

Remark 4.7. Applying an R4 move to a spatial surface diagram changes the framing of an edge. There is a possibility that an R5 move changes the framing of an edge.

We denote by R1- the Reidemeister move R1 that reduces the number of crossings.

Lemma 4.8. *Let $(D_i)_{1 \leq i \leq n}$ be a sequence of spatial surface diagrams such that*

- D_1 and D_n have no bivalent vertices and
- D_i is transformed into D_{i+1} by an R0 move or an R1- move for any i .

Then, D_1 and D_n are related by $R\omega$ and R2–R3 moves in \mathbb{R}^2 .

Proof. By our assumption, we see that D_1 is obtained by continuing to replace an local arc of D_n with a teardrop-like piece, see Figure 31. On each edge of D_1 , we move teardrop-like pieces into a small region so that all the teardrop-like pieces of an edge are aligned as depicted in Figure 32. When a teardrop-like piece is passing through a crossing, R2–R3 moves are applied, see Figure 33. By the process, we have a new spatial surface diagram D'_1 such that D'_1 and D_1 are related by R2–R3 moves.

We show that D_n and D'_1 are related by $R\omega$ and R2–R3 moves; then the proof will be shown. Since D_1 and D_n are related by R0–R1 moves, D'_1 and D_n are related by R0–R3 moves. By Lemma 4.6, the framing of each edge does not change before and after the process above. Therefore, in each local area where the teardrop-like pieces are gathered, the number of positive self-crossings is equal to that of negative self-crossings. In Figure 32, the B and C parts are canceled by R2–R3 moves by Lemma 4.4 (1), and the A and D parts are also canceled by $R\omega$ moves by Lemma 4.4 (2). Hence, D_n and D'_1 are related by $R\omega$ and R2–R3 moves. \square



FIGURE 31. A teardrop-like piece

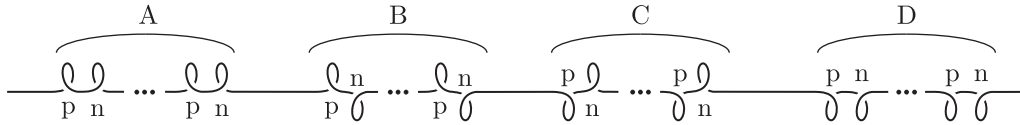


FIGURE 32. The symbols “p” and “n” mean positive and negative self-crossings, respectively.

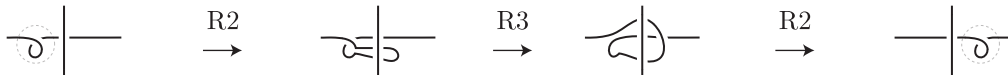


FIGURE 33. Deformations by R2–R3 moves

The lemma below follows immediately.

Lemma 4.9. *Let D and D' be spatial surface diagrams. We suppose that D has no bivalent vertices. If D and D' are related by R0, R2–R3 and R5 moves in \mathbb{R}^2 , then D and $\overline{D'}$ are related by R2–R3 and R5 moves in \mathbb{R}^2 , and $\overline{D'}$ and D' are related by R0 moves.*

Proposition 4.10. *Let D and D' be spatial surface diagrams that have no signs. If D and D' are related by R0–R3 and R5 moves in \mathbb{R}^2 , then D and D' are related by $R\omega$, R2–R3, and R5 moves in \mathbb{R}^2 .*

Proof. It suffices to construct a spatial surface diagram D'' with no bivalent vertices such that D and D'' are related by R2–R3 and R5 moves and that D'' and D' are related by $R\omega$, R2–R3, and R5 moves.

Since D and D' are related by R0–R3 and R5 moves, we fix a sequence $(D_i)_{1 \leq i \leq n}$ of spatial surface diagrams related by R0–R3 and R5 moves such that $D_1 = D$ and $D_n = D'$. Modifying the sequence $(D_i)_{1 \leq i \leq n}$, we will recursively construct a new sequence $(D'_i)_{1 \leq i \leq n}$ of spatial surface diagrams satisfying that D'_i and D'_{i+1} are related by R0, R2–R3 and R5 moves for every i with $1 \leq i < n$. We set $D'_1 = D_1$. Suppose that D'_i is already defined.

Case 1: we consider the case where D_i and D_{i+1} are related by an R1 move. We suppose that the left R1 move in Figure 14 is applied. As is illustrated in Figure 34, we define D'_{i+1} for two cases: we attach a “small bivalent disk” on spatial surface diagrams, in stead of applying the left R1 move in Figure 14. Each small bivalent disk contains one teardrop-like part and two bivalent vertices. At a glance, D'_i and D'_{i+1} seem to be related by an R1 move. However, D'_i and D'_{i+1} are actually related by R0 and R2 moves. If a small bivalent disk attached to D'_i is contained in the region where an R1 move is applied, we move it into on the outside of the region by using R0 and R2–R3 moves before we define D'_{i+1} , see Figure 35. For also the right R1 move in Figure 14, we define D'_{i+1} in the same manner.

Case 2: we consider the case where D_i and D_{i+1} are related by one of R0, R2–R3 and R5 moves. Let $\delta \subset \mathbb{R}^2$ be a disk in which the moves is applied. If a small bivalent disk attached to D'_i is contained in δ , we move it on the outside of δ by using R0 and R2–R3 moves before we define D'_{i+1} , as is the case 1. We define D'_{i+1} as follows: D'_{i+1} is equal to D'_i in the outside of δ and the part of D'_{i+1} contained in δ corresponds to the applied move.

By the above definitions, we obtain a sequence $(D'_i)_{1 \leq i \leq n}$ such that D'_i and D'_{i+1} are related by R0, R2–R3 and R5 moves for any i . Then, $D(= D'_1 = D_1)$ and D'_n are related by R0, R2–R3 and R5 moves. Hence, by Lemma 4.9, (i) the spatial surface diagrams D and $D'' := \overline{D'_n}$ are related by R2–R3 and R5 moves, and D'' and D'_n are related by R0 moves. On the other hand, D'_n is transformed into $D'(= D_n)$ by using R0 and R1- moves in each small bivalent disk. Then, D'' is also transformed into D' by using R0 and R1- moves. By Lemma 4.8, we understand that (ii) D'' and D' are related by $R\omega$, R2–R3 and R5 moves in \mathbb{R}^2 . By using (i) and (ii), D and D' are related by $R\omega$, R2–R3 and R5 moves. \square

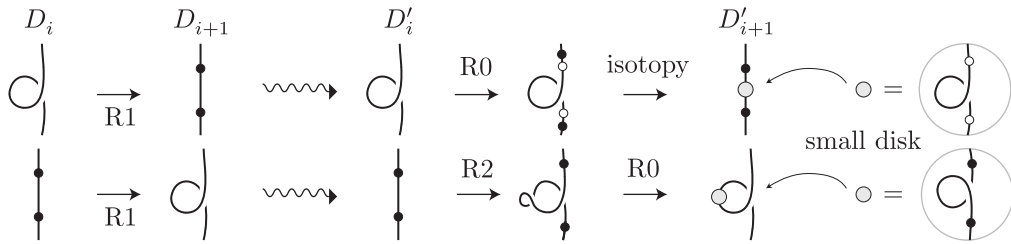


FIGURE 34. Replace an R1 move with R0 and R2 moves.

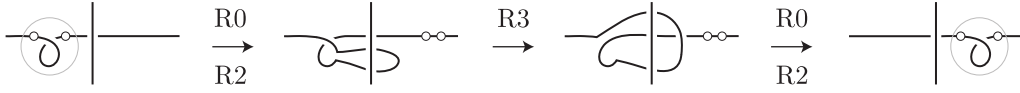


FIGURE 35. This move is realized by R0 and R2–R3 moves.

We denote by $R4^-$ the Reidemeister move R4 that reduces the number of crossings.

Lemma 4.11. *Let $(D_i)_{1 \leq i \leq n}$ be a sequence of spatial surface diagrams satisfying that*

- D_i is transformed into D_{i+1} by an $R4^-$ move for any i , and
- $R4^-$ moves are applied an even number of times at each trivalent vertex in $(D_i)_{1 \leq i \leq n}$.

Then, D_1 and D_n are related by R0–R3 and R5 moves in \mathbb{R}^2 .

Proof. It is sufficient to prove that D_1 and D_n are related by R0–R3 and R5 moves if $R4^-$ moves are applied exactly two times at each vertex v in $(D_i)_{1 \leq i \leq n}$. All situations around a trivalent vertex of D_1 are depicted in Figure 36: each local part in the figure is transformed into a Y-shaped part by using two $R4^-$ moves.

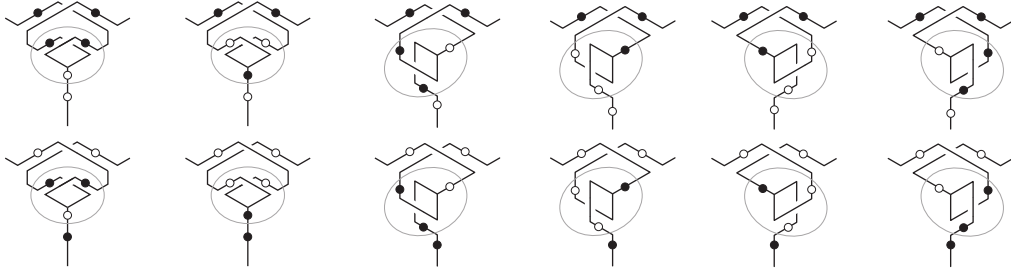


FIGURE 36. All situations around a trivalent vertex

As is depicted in Figure 37, the upper left of Figure 36 is deformed into a Y-shaped part by using R0–R3, R5 moves. Similarly, each of Figure 36 is deformed into a Y-shaped part by using R0–R3, R5 moves, although its process is not depicted. \square

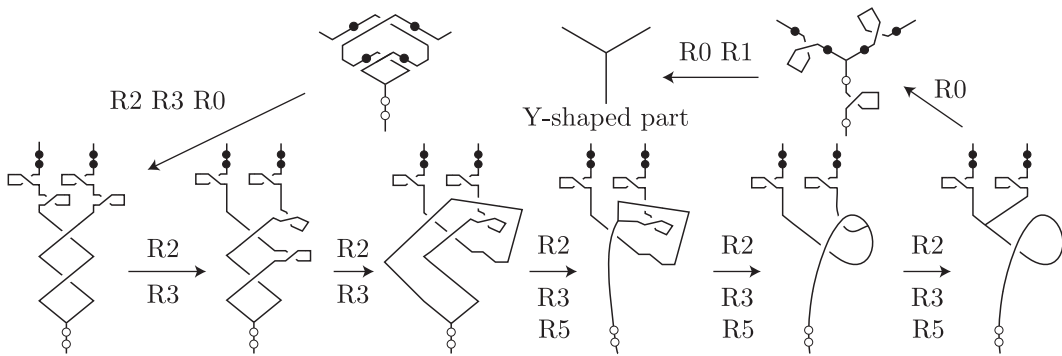


FIGURE 37. A deformation into a Y-shaped part by R0–R3 and R5 moves

Proposition 4.12. *Let $(D_i)_{1 \leq i \leq n}$ be a sequence of spatial surface diagrams satisfying that*

- both D_1 and D_n have no bivalent vertices,
- D_i and D_{i+1} are related by one of R0–R5 moves for any i , and
- $R4^-$ moves are applied an even number of times at each trivalent vertex in $(D_i)_{1 \leq i \leq n}$.

Then, D_1 and D_n are related by $R\omega, R2-R3$ and $R5$ moves in \mathbb{R}^2 .

Proof. We will show that D_1 and D_n are related by $R0-R3$ and $R5$ moves; then D_1 and D_n are related by $R\omega, R2-R3$ and $R5$ moves by Proposition 4.10, that is, the proof will complete. It suffices to construct a sequence $(D'_i)_{1 \leq i \leq n+m}$ of spatial surface diagrams with $D'_1 = D_1$ and $D'_{n+m} = D_n$ satisfying that

- (i) D'_i and D'_{i+1} are related by $R0-R3$ and $R5$ moves for any integer $1 \leq i < n$,
- (ii) D'_i is transformed into D'_{i+1} by an $R4^-$ move for any integer i with $n \leq i < n+m$,
- (iii) $R4^-$ moves are applied an even number of times at each trivalent vertex in $(D'_i)_{n \leq i \leq n+m}$,

since D'_n and D'_{m+n} are related by $R0-R3$ and $R5$ moves by Lemma 4.11.

First, by modifying the given sequence $(D_i)_{1 \leq i \leq n}$, we recursively construct a sequence $(D'_i)_{1 \leq i \leq n}$ of spatial surface diagrams. We set $D'_1 := D_1$. Suppose that D'_i is already defined.

Case 1: we consider the case where D_i and D_{i+1} are related by an $R4$ move. Suppose that the left $R4$ move in Figure 14 is applied. Let v be the trivalent vertex in which the move is applied. We define D'_{i+1} as illustrated in Figure 38: we replace v in D'_i with a “small trivalent disk”, instead of applying the left $R4$ move in Figure 38. Each small trivalent disk contains a trivalent vertex and three bivalent vertices. At a glance, D'_i and D'_{i+1} seem to be related by an $R4$ move. However, D'_i and D'_{i+1} are actually related by $R0$ and $R2$ moves. If a trivalent vertex is already replaced with a small trivalent disk, we think of the trivalent disk as a trivalent vertex. In the case, the small trivalent disk contains a smaller trivalent disk. For the case where the right $R4$ move in Figure 14 is applied, we define D'_{i+1} in the same manner.

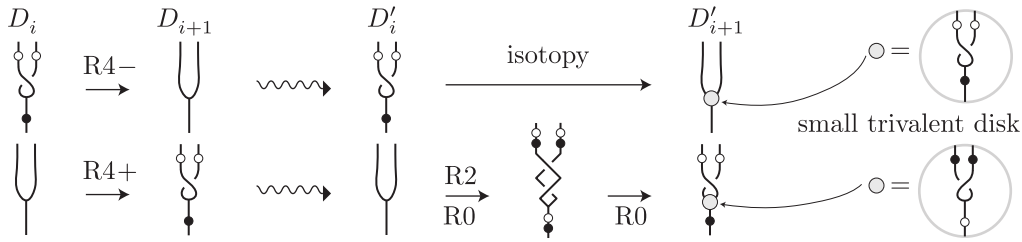


FIGURE 38. A trivalent vertex is replaced by a “small trivalent disk”.

Case 2: we consider the case where D_i and D_{i+1} are related by an $R0-R3$ or $R5$ move. Suppose that an $R0, R1, R2$ or $R3$ move is applied in a region δ . We define the spatial surface diagram D'_{i+1} as follows: D'_{i+1} is equal to D'_i on the outside of δ , and D'_{i+1} is equal to D_{i+1} on the inside of δ . Suppose that an $R5$ move is applied in a region δ . If δ contains no trivalent small disk, we define D'_{i+1} in the same way above. If δ contains trivalent small disks, we regard the outermost small trivalent disk as a trivalent vertex and define D'_{i+1} in the same way above. In this case, D'_{i+1} and D'_i are related by $R0, R2-R3$ and $R5$ moves, see Figure 39.

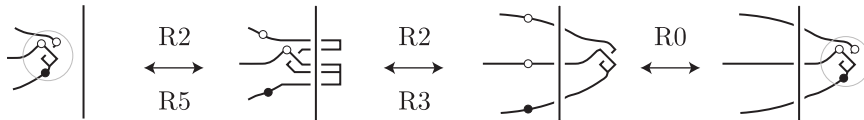


FIGURE 39. An $R5$ move at a small trivalent disk is realized by $R0, R2-R3$ and $R5$ moves.

By the construction above, (i) holds.

Secondly, we construct a sequence $(D'_i)_{n \leq i \leq n+m}$ of spatial surface diagrams. We continue applying $R4^-$ moves in order starting from the innermost small trivalent disks of D'_n , until trivalent disks disappear. We have D_n , finally. Let $(D'_i)_{n \leq i \leq n+m}$ be a sequence obtained by the above

process satisfying that $D'_{n+m} = D_n$ and the condition (ii). The number of R4 moves in $(D_i)_{1 \leq i \leq n}$ is equal to the number of R4⁻ moves in $(D'_i)_{n \leq i \leq n+m}$ at each trivalent vertex. Since R4 moves are applied an even number of times at each trivalent vertex in $(D_i)_{1 \leq i \leq n}$, then the condition (iii) holds. \square

Proof of Theorem 3.5. Since F and $\overrightarrow{\text{Sf}}(D)$ are ambient isotopic, we assume that $F = \overrightarrow{\text{Sf}}(D)$. For the same reason, we assume that $F' = \overrightarrow{\text{Sf}}(D')$.

We suppose that (b) holds; we show that (c) holds. By Lemma 4.4 (2), an $R\omega$ move is realized by R2–R3 and R5 moves in S^2 ; then (c) holds.

We suppose that (c) holds; we show that (a) holds. If D and D' are related by exactly one of R2–R3 and R5–R6 moves, we can immediately construct an isotopy between F and F' that preserves the orientations of F and F' . Since D and D' are related by finitely many R2–R3 and R5–R6 moves, then F and F' are also ambient isotopic including orientations: (a) holds.

We suppose that (a) holds; we show that (b) holds. Let G (resp. G') be the trivalent spine of F (resp. F') such that $D(G; F) = D$ (resp. $D(G'; F') = D'$). Since F and F' are ambient isotopic including orientations, we fix an isotopy $\{h_t : \mathbb{R}^3 \rightarrow \mathbb{R}^3\}_{t \in [0,1]}$ with $h_0 = \text{id}|_{\mathbb{R}^3}$ such that $h_1(F) = F'$ including orientations, and that $(h_1(G); h_1(F))$ is in regular position. By Lemma 4.3 (2), $D(h_1(G); h_1(F))$ and D' are related by R2–R3 and R5–R6 moves in \mathbb{R}^2 . Then, it suffices to show that D and $D(h_1(G); h_1(F))$ are related by $R\omega$, R2–R3 and R5 moves in \mathbb{R}^2 . By Lemma 4.2, D and $D(h_1(G); h_1(F))$ are related by R0–R5 moves. Let $(D_i)_{1 \leq i \leq n}$ be a sequence of spatial surface diagrams with $D_1 = D$ and $D_n = D(h_1(G); h_1(F))$ such that D_i and D_{i+1} are related by one of R0–R5 moves for any i , where we note that both D_1 and D_n have no bivalent vertices. Since the orientation of the oriented spatial surface F is equal to that of the oriented spatial surface F' , then R4 moves are applied an even number of times at each trivalent vertex in $(D_i)_{1 \leq i \leq n}$. Hence, $(D_i)_{1 \leq i \leq n}$ satisfies all of the conditions in Proposition 4.12. By Proposition 4.12, D_1 and D_n are related by $R\omega$, R2–R3 and R5 moves. \square

5. A DIAGRAM OF A NON-SPLIT SPATIAL SURFACE

In Sections 3 and 4, we called a spatial surface with boundary a spatial surface for short. In this section, we use the notion of a spatial surface in the original definition: a spatial surface may have some closed components, see Section 3. We assume that a spatial surface has no sphere components and no disk components, since a sphere or disk in S^3 is unique up to ambient isotopy.

A spatial surface S is *split* if there is a 2-sphere P embedded in $S^3 \setminus \text{int } S$ such that P bounds no balls in $S^3 \setminus \text{int } S$. A spatial surface S is *non-split* if S is not split, that is, any sphere embedded in $S^3 \setminus \text{int } S$ bounds a ball. We note that any 1-component spatial surface is always non-split.

In this section, we consider a way to present non-split spatial surfaces. Let S be a non-split spatial surface. If S has closed components S_1, \dots, S_n , we remove the interior of a disk δ_i from S_i . By the finitely many operations of removing a disk interior in each closed component, we have a spatial surface $F := S \setminus \text{int } \delta$ with boundary, where we put $\delta = \delta_1 \sqcup \dots \sqcup \delta_n$. Proposition 5.1 claims that F has necessary and sufficient information of the original spatial surface S up to ambient isotopy. Therefore, when we deal with a spatial surface that has closed components, it is sufficient to consider a spatial surface with boundary that is obtained from the original spatial surface by removing a disk interior of each closed component.

Proposition 5.1. *Let S be a non-split spatial surface, and let $\delta := \delta_1 \sqcup \dots \sqcup \delta_n$ be a disjoint union of disks in $\text{int } S$. We denote by F the non-split spatial surface $S \setminus \text{int } \delta$. Let $\Delta := \Delta_1 \sqcup \dots \sqcup \Delta_n$ be a disjoint union of disks in $S^3 \setminus \text{int } F$ such that $\partial\Delta_i = \partial\delta_i$ for any integer i with $1 \leq i \leq n$. Then, the spatial surfaces S and $F \cup \Delta$ are ambient isotopic in S^3 .*

Proof. We use the Cut-And-Paste method. By an isotopy of $S^3 \setminus \text{int } F$, we deform Δ so that $|L|$ is minimal, where we put $L = \text{int } \delta \cap \text{int } \Delta$, and $|L|$ is the number of connected components of L .

We show that $L = \emptyset$; we suppose that $L \neq \emptyset$. We may assume that every connected component of L is a loop. We take an innermost disk δ_0 on δ , where we note $\Delta \cap \text{int } \delta_0 = \emptyset$ and $\partial\delta_0$ is a loop in L . Put $l_0 = \partial\delta_0$. Let Δ_0^+ be the disk on Δ such that $\partial\Delta_0^+ = l_0$. Let A be a thin regular neighborhood of l_0 in Δ , where we note that A is an annulus in Δ . Let l^+ (resp. l^-) be the loop

of ∂A such that $l^+ \subset \Delta_0^+$ (resp. $l^- \subset \Delta \setminus \Delta_0^+$). Let δ^+ (resp. δ^-) be a disk in $S^3 \setminus S$ such that δ^+ (resp. δ^-) is parallel to δ_0 and $\partial\delta^+ = l^+$ (resp. $\partial\delta^- = l^-$). Put $\Delta^- = (\Delta \setminus \Delta_0^+ \setminus A) \cup \delta^-$. Since F is non-split, the sphere $(\Delta_0^+ \setminus A) \cup \delta^+$ bounds a ball in $S^3 \setminus \text{int } F$. Then, $F \cup \Delta$ and $F \cup \Delta^-$ are ambient isotopic in $S^3 \setminus \text{int } F$. On the other hand, $|L'|$ is less than $|L|$, where we put $L' = \text{int } \Delta^- \cap \text{int } \delta$. This leads to a contradiction with the minimality of $|L|$. Hence, $L = \emptyset$.

We put $P_i = \delta_i \cup \Delta_i$ for any integer i with $1 \leq i \leq n$, where we note that $\Delta \cup \delta = P_1 \sqcup \cdots \sqcup P_n$ is a disjoint union of spheres embedded in $S^3 \setminus \text{int } F$. Since F is non-split, each sphere P_i bounds a ball B_i in $S^3 \setminus \text{int } F$; then $F \cap \text{int } B_i = \emptyset$. Let i and j be integers with $i \neq j$. If $B_j \subset \text{int } B_i$, it holds that $\partial\delta_j \subset P_j = \partial B_j \subset \text{int } B_i$, and we have $F \cap \text{int } B_i \neq \emptyset$, since $\partial\delta_j \subset F$. This leads to a contradiction. Hence, we have $B_j \not\subset \text{int } B_i$, that is, $B_i \cap B_j = \emptyset$; therefore the balls B_1, \dots, B_n are pairwise disjoint.

In each ball B_i , we deform Δ_i into δ_i by an isotopy of $S^3 \setminus \text{int } F$. Therefore, the spatial surfaces $F \cup \delta$ and $F \cup \Delta$ are ambient isotopic in S^3 , where we note that $F \cup \delta = S$. \square

In Proposition 5.1, if S is split, the claim does not always hold because there is no information about a ‘‘partition’’ of S^3 by the closed components of S .

Theorem 5.2. *Let S (resp. S') be a non-split unoriented spatial surface. Let F (resp. F') be the non-split unoriented spatial surface with boundary that is obtained from S (resp. S') by removing an open disk from every closed component. Let D (resp. D') be a diagram of F (resp. F'). Then, the following conditions are equivalent.*

- (a) S and S' are ambient isotopic in S^3 .
- (b) D and D' are related by R0–R6 moves in \mathbb{R}^2 .

Proof. Suppose that (a) is satisfied. We show that (b) holds. Let δ (resp. δ') be a disjoint union of disks contained in S (resp. S') such that $F = S \setminus \text{int}(\delta)$ (resp. $F' = S' \setminus \text{int}(\delta')$). Since S and S' are ambient isotopic in S^3 , we take an isotopy $\{h_t : S^3 \rightarrow S^3\}_{t \in [0,1]}$ such that $h_0 = \text{id}|_{S^3}$ and $h_1(S) = S'$. Then, F and $S' \setminus \text{int } h_1(\delta)$ are ambient isotopic in S^3 . On the other hand, since $h_1(\delta)$ and δ' are ambient isotopic in S' , the spatial surfaces $S' \setminus \text{int } h_1(\delta)$ and F' are ambient isotopic in S' ; then $S' \setminus \text{int } h_1(\delta)$ and F' are also ambient isotopic in S^3 . Therefore, F and F' are ambient isotopic in S^3 . By Theorem 3.4, D and D' are related by R0–R6 moves in \mathbb{R}^2 .

Suppose that (b) is satisfied. By Theorem 3.4, F and F' are ambient isotopic in S^3 . Since F and F' are non-split, S and S' are ambient isotopic in S^3 by Proposition 5.1: (a) is satisfied. \square

In the same manner, we have Theorem 5.3 below by using Theorem 3.5 and Proposition 5.1.

Theorem 5.3. *Let S (resp. S') be a non-split oriented spatial surface. Let F (resp. F') be the non-split oriented spatial surface with boundary that is obtained from S (resp. S') by removing an open disk from every closed component. Let D (resp. D') be a diagram of F (resp. F'). Then, the following conditions are equivalent.*

- (a) S and S' are ambient isotopic in S^3 including orientations.
- (b) D and D' are related by $R\omega$, R2–R3 and R5–R6 moves in \mathbb{R}^2 .
- (c) D and D' are related by R2–R3 and R5–R6 moves in S^2 .

Next, we explain relations among knots, handlebody-knots and spatial surfaces. For a manifold X embedded in S^3 , we denote by $[X]$ the ambient isotopy class of X in S^3 . We put

$$\begin{aligned} \mathcal{K} &= \{[K] \mid K \text{ is a non-split link}\}, \\ \mathcal{H} &= \{[H] \mid H \text{ is a non-split handlebody-link}\}, \\ \mathcal{S}_{\text{cl}} &= \{[S] \mid S \text{ is a non-split spatial closed surface}\}, \\ \mathcal{F}_{\text{or}} &= \{[F] \mid F \text{ is a non-split orientable spatial surface with boundary}\}, \end{aligned}$$

where we note that a knot is a kind of non-split link, and a handlebody-knot is kind of non-split handlebody-link. The following maps are injective:

$$f_1 : \mathcal{K} \rightarrow \mathcal{H}; [K] \mapsto [N_K], \quad f_2 : \mathcal{H} \rightarrow \mathcal{S}_{\text{cl}}; [H] \mapsto [\partial H], \quad f_3 : \mathcal{S}_{\text{cl}} \rightarrow \mathcal{F}_{\text{or}}; [S] \mapsto [F_S],$$

where N_K means a regular neighborhood of K in S^3 , and F_S means a spatial surface with boundary obtained from S by removing the interior of a disk in each closed component of S . Injectivity of f_3 follows from Proposition 5.1.

By injectivity of the above maps, we have new presentation of non-split links and non-split handlebody-links by using spatial surface diagrams, see Figure 40. This suggests a new approach to studying a knot, link, handlebody-knot and handlebody-link in a framework of spatial surfaces.

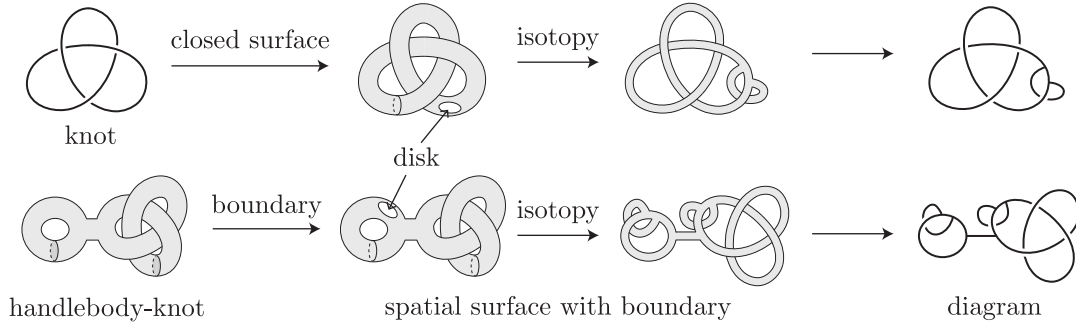


FIGURE 40. Presentation of knots and handlebody-knots by using spatial surface diagrams

Remark 5.4. The map f_2 above is not surjective. There are infinitely many spatial closed surfaces that bounds no handlebody-knots up to ambient isotopy. The spatial closed surface S of Figure 41 bounds no handlebodies: each fundamental group of connected components of $S^3 \setminus S$ is not free (cf. [3]).

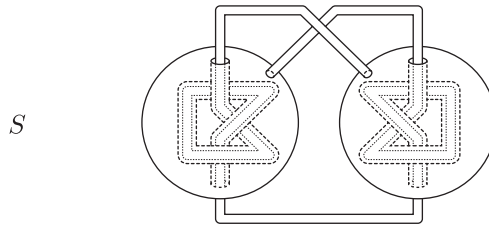


FIGURE 41. A spatial closed surface with genus 2 that bounds no handlebody-knots

REFERENCES

- [1] N. Apostolakis, R. Piergallini and D. Zuddas, *Lefschetz fibrations over the disk*, Proc. London Math. Soc. **107** (2013), 240–290.
- [2] I. Bobtcheva and R. Piergallini, *On 4-dimensional 2-handlebodies and 3-manifolds*, J. Knot Theory Ramifications **21** (2012), no. 12, 1250110.
- [3] T. Homma, *On the existence of unknotted polygons on 2-manifolds in E^3* , Osaka J. Math. **6** (1954), 129–134.
- [4] A. Ishii, *Moves and invariants for knotted handlebodies*, Algebr. Geom. Topol. **8** (2008), 1403–1418.
- [5] L. H. Kauffman, *Invariants of graphs in three-space*, Trans. Am. Math. Soc. **311** (1989), no. 2, 2788–2794.
- [6] F. Luo, *On heegaard diagrams*, Math. Res. Lett. **4** (1997), 365–373.
- [7] K. Reidemeister, *Knotten und Gruppen*, Abh. Math. Sem. Univ. Hamburg **5** (1927), 7–23.
- [8] D. Roseman, *Reidemeister-type moves for surfaces in four-dimensional space*, In: “Knot theory”, Banach Center Publ. **42**, Polish Acad. Sci. Inst. Math. Warsaw, 1998, 347–380.
- [9] S. Suzuki, *On complexity of a surface in 3-sphere*, Osaka J. Math. **11** (1974), 113–127.
- [10] Y. Tsukui, *On surfaces in 3-space*, Yokohama Math. J. **18** (1970), 93–104.

LEARNING SUPPORT CENTER, FACULTY OF ENGINEERING, TAKUSHOKU UNIVERSITY, 815-1 TATEMACHI, HACHIOJISHI, TOKYO, 193-0985, JAPAN

E-mail address: smatsuz@ner.takushoku-u.ac.jp